

Nucleophilic substitution reactions at the Si–Cl bonds of the dichloro(methyl)silyl ligand in five- and six-coordinate complexes of ruthenium(II) and osmium(II)

Wai-Him Kwok, Guo-Liang Lu, Clifton E.F. Rickard, Warren R. Roper*,
L. James Wright*

Department of Chemistry, The University of Auckland, Private Bag 92019, Auckland, New Zealand

Received 4 March 2004; accepted 15 April 2004

Abstract

Treatment of either $\text{RuHCl}(\text{CO})(\text{PPh}_3)_3$ or $\text{MPhCl}(\text{CO})(\text{PPh}_3)_2$ with HSiMeCl_2 produces the five-coordinate dichloro(methyl)silyl complexes, $\text{M}(\text{SiMeCl}_2)\text{Cl}(\text{CO})(\text{PPh}_3)_2$ (**1a**, $\text{M} = \text{Ru}$; **1b**, $\text{M} = \text{Os}$). **1a** and **1b** react readily with hydroxide ions and with ethanol to give $\text{M}(\text{SiMe}[\text{OH}]_2)\text{Cl}(\text{CO})(\text{PPh}_3)_2$ (**2a**, $\text{M} = \text{Ru}$; **2b**, $\text{M} = \text{Os}$) and $\text{M}(\text{SiMe}[\text{OEt}]_2)\text{Cl}(\text{CO})(\text{PPh}_3)_2$ (**3a**, $\text{M} = \text{Ru}$; **3b**, $\text{M} = \text{Os}$), respectively. **3b** adds CO to form the six-coordinate complex, $\text{Os}(\text{SiMe}[\text{OEt}]_2)\text{Cl}(\text{CO})_2(\text{PPh}_3)_2$ (**4b**) and crystal structure determinations of **3b** and **4b** reveal very different Os–Si distances in the five-coordinate complex (2.3196(11) Å) and in the six-coordinate complex (2.4901(8) Å). Reaction between **1a** and **1b** and 8-aminoquinoline results in displacement of a triphenylphosphine ligand and formation of the six-coordinate chelate complexes $\text{M}(\text{SiMeCl}_2)\text{Cl}(\text{CO})(\text{PPh}_3)(\kappa^2(N,N)\text{-NC}_9\text{H}_6\text{NH}_2\text{-}8)$ (**5a**, $\text{M} = \text{Ru}$; **5b**, $\text{M} = \text{Os}$), respectively. Crystal structure determination of **5a** reveals that the amino function of the chelating 8-aminoquinoline ligand is located adjacent to the reactive Si–Cl bonds of the dichloro(methyl)silyl ligand but no reaction between these functions is observed. However, **5a** and **5b** react readily with ethanol to give ultimately $\text{M}(\text{SiMe}[\text{OEt}]_2)\text{Cl}(\text{CO})(\text{PPh}_3)(\kappa^2(N,N)\text{-NC}_9\text{H}_6\text{NH}_2\text{-}8)$ (**6a**, $\text{M} = \text{Ru}$; **6b**, $\text{M} = \text{Os}$). In the case of ruthenium only, the intermediate ethanolsis product $\text{Ru}(\text{SiMeCl}[\text{OEt}])\text{Cl}(\text{CO})(\text{PPh}_3)(\kappa^2(N,N)\text{-NC}_9\text{H}_6\text{NH}_2\text{-}8)$ (**6c**) was also isolated. The crystal structure of **6c** was determined. Reaction between **1b** and excess 2-aminopyridine results in condensation between the Si–Cl bonds and the N–H bonds with formation of a novel tridentate “NSiN” ligand in the complex $\text{Os}(\kappa^3(\text{Si},N,N)\text{-SiMe}[\text{NH}(2\text{-C}_3\text{H}_4\text{N})_2])\text{Cl}(\text{CO})(\text{PPh}_3)$ (**7b**). Crystal structure determination of **7b** shows that the “NSiN” ligand coordinates to osmium with a “facial” arrangement and with chloride *trans* to the silyl ligand.

© 2004 Elsevier B.V. All rights reserved.

Keywords: Silyl complex; Osmium; Ruthenium; X-ray crystal structure; Tridentate ligand

1. Introduction

Metal complexes with chloro-substituted silyl ligands, $\text{L}_n\text{M-SiR}_{3-n}\text{Cl}_n$ ($n = 1\text{--}3$), have proved to be useful substrates, through nucleophilic substitution reactions, for the syntheses of silyl complexes with interesting functionalisation at silicon. Examples include the syntheses of

compounds of the type, $\text{L}_n\text{M-SiR}_{3-n}\text{X}_n$, where X can be H [1], R [2], OH [3,4], OR [5], SR [6], NR_2 [7], and F [8,2]. Furthermore, several complexes containing the dimethylamino-bridged bis(silylene) ligand system, have been prepared directly from reaction between $\text{HSiMe}_2\text{NMe}_2$ and chlorodimethylsilyl complexes of ruthenium(II) and osmium(II) in complex reactions in which one step may involve a nucleophilic substitution at silicon [9]. The reactivity of the Si–Cl bonds in all chlorosilyl ligands is variable and in some cases the Si–Cl bonds are quite unreactive towards hydrolysis.

* Corresponding authors. Tel.: +64-9-373-7999x8320; fax: +64-9-373-7422.

E-mail address: w.roper@auckland.ac.nz (W.R. Roper).

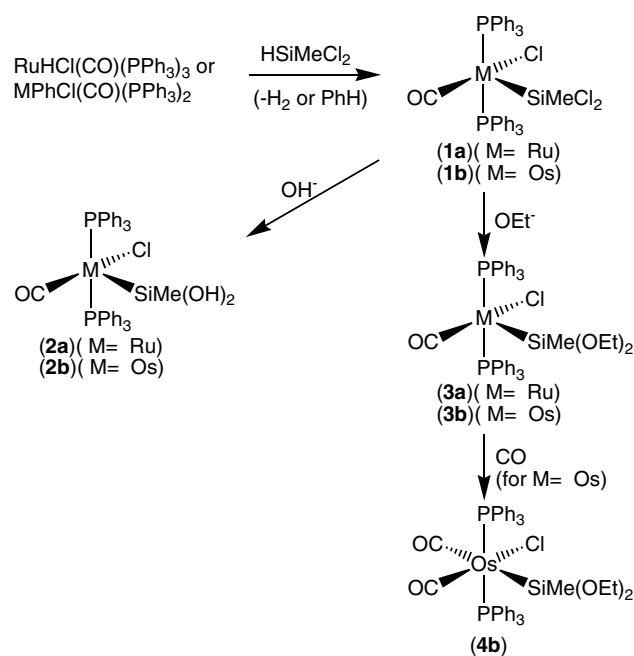
An instance is provided by the ready hydrolysis of $\text{CpFe}(\text{CO})_2\text{SiR}_2\text{Cl}$ whereas the corresponding ruthenium derivative, $\text{CpRu}(\text{CO})_2\text{SiR}_2\text{Cl}$, is inert to hydrolysis [10]. Two $\text{CpFe}(\text{CO})_2$ fragments attached to the one silicon atom in $[\text{CpFe}(\text{CO})_2]_2\text{SiCl}_2$ renders the Si–Cl bonds unreactive to Cl/OH exchange [11]. Additionally, the number of halide substituents on the silyl ligand affects the reactivity, e.g., when one of the chlorides in $[\text{CpFe}(\text{CO})_2]_2\text{SiCl}_2$ is replaced by hydride to give $[\text{CpFe}(\text{CO})_2]_2\text{SiHCl}$ the remaining Si–Cl bond is readily hydrolysed. Interestingly, structural data suggests that both the Ru–Si and Si–Cl distances in $\text{Cp}(\text{PR}_3)_2\text{RuSiX}_3$ increase when chloride is replaced by either methyl or phenyl [12]. The increased Si–Cl distances have been attributed to $d(\text{Ru})-\sigma^*(\text{Si}-\text{Cl})$ π -back-bonding interactions and this may partly explain the increased Si–Cl bond reactivity. To contribute to further understanding of the reactivity of chloro-substituted silyl ligands we have developed convenient routes to dichloro(methyl)silyl complexes of both ruthenium(II) and osmium(II) and examined some features of their chemistry.

Herein, we report (i) the syntheses of the dichloro(methyl)silyl complexes, $\text{M}(\text{SiMeCl}_2)\text{Cl}(\text{CO})(\text{PPh}_3)_2$ (**1a**, $\text{M} = \text{Ru}$; **1b**, $\text{M} = \text{Os}$), (ii) the hydrolysis and ethanolation of the silyl ligands in these complexes, (iii) the carbonylation of $\text{Os}[\text{SiMe}(\text{OEt})_2]\text{Cl}(\text{CO})(\text{PPh}_3)_2$ (**3b**) to give $\text{Os}[\text{SiMe}(\text{OEt})_2]\text{Cl}(\text{CO})_2(\text{PPh}_3)_2$ (**4b**), (iv) a comparison of the crystal structures of **3b** and **4b**, (v) the reaction of **1a** and **1b** with 8-aminoquinoline to give $\text{M}(\text{SiMeCl}_2)\text{Cl}(\text{CO})(\text{PPh}_3)(\kappa^2(N,N\text{-NC}_9\text{H}_6\text{NH}_2\text{-}8))$ (**5a**, $\text{M} = \text{Ru}$ (structurally characterized); **5b**, $\text{M} = \text{Os}$) with unchanged dichloro(methyl)silyl ligands and triphenylphosphine displacement, and (vi) the reaction of **1b** with 2-aminopyridine to give $\text{Os}(\kappa^3(\text{Si},N,N)\text{-SiMe}[\text{NH}(\text{C}_5\text{H}_4\text{N})_2]\text{Cl}(\text{CO})(\text{PPh}_3))$ (**7b**) (structurally characterized) with formation of a novel “NSiN” tridentate silyl ligand through reaction at both Si–Cl bonds.

2. Results and discussion

2.1. Syntheses of the dichloro(methyl)silyl complexes, $\text{M}(\text{SiMeCl}_2)\text{Cl}(\text{CO})(\text{PPh}_3)_2$ (**1a**, $\text{M} = \text{Ru}$; **1b**, $\text{M} = \text{Os}$) and subsequent reactions with water and ethanol

We have demonstrated that a simple and convenient route to coordinatively unsaturated silyl complexes of ruthenium(II) and osmium(II) of general formula $\text{M}(\text{SiR}_3)\text{Cl}(\text{CO})(\text{PPh}_3)_2$ involves reaction between a silane, H-SiR_3 , and $\text{MPhCl}(\text{CO})(\text{PPh}_3)_2$. For $\text{M} = \text{Ru}$, and for certain silanes, an alternative substrate is $\text{RuHCl}(\text{CO})(\text{PPh}_3)_3$. Successful reactions have been achieved for $\text{SiR}_3 = \text{SiCl}_3$ [5,3], SiMe_3 [5], SiEt_3 [5], SiMe_2Cl [13,14], $\text{Si}(\text{pyrrolyl})_3$ [15], $\text{Si}(\text{OEt})_3$ [16], and $\text{Si}(\text{OC}_2\text{H}_4)_3\text{N}$ [17,18]. We now report that reactions utilizing H-SiMeCl_2 as the silane are equally successful. As de-



Scheme 1. Syntheses and reactions of dichloro(methyl)silyl complexes of ruthenium(II) and osmium(II).

icted in Scheme 1, reaction between $\text{MPhCl}(\text{CO})(\text{PPh}_3)_2$ (or $\text{RuHCl}(\text{CO})(\text{PPh}_3)_3$) and excess H-SiMeCl_2 , leads cleanly to $\text{M}(\text{SiMeCl}_2)\text{Cl}(\text{CO})(\text{PPh}_3)_2$ (**1a**, $\text{M} = \text{Ru}$; **1b**, $\text{M} = \text{Os}$). The IR spectrum (Nujol mull) of yellow $\text{Ru}(\text{SiMeCl}_2)\text{Cl}(\text{CO})(\text{PPh}_3)_2$ has absorptions assigned to $\nu(\text{CO})$ at 1953, 1936, 1923 cm^{-1} and the corresponding bands for the yellow-orange osmium analogue occur at 1942, 1925, 1911 cm^{-1} (full spectroscopic data for these and all other new compounds are in Section 4). Although these compounds are mono-carbonyl, the multiple carbonyl absorptions observed are attributed to solid-state splitting. This same phenomenon was also observed for the hydrolysis products **2a** and **2b** to be described below. The other mono-carbonyl compounds described in this paper all showed the expected single $\nu(\text{CO})$. Despite the splitting of these bands for **1a** and **1b** it is clear that the absorptions for the osmium compound are lower than those for the ruthenium compound.

Treatment of the dichloro(methyl)silyl complexes, **1a** and **1b**, with excess K_2CO_3 suspended in a THF/ H_2O mixture leads rapidly to the formation of the yellow dihydroxy(methyl)silyl complexes, $\text{Ru}(\text{SiMe}[\text{OH}]_2)\text{Cl}(\text{CO})(\text{PPh}_3)_2$ (**2a**) and $\text{Os}(\text{SiMe}[\text{OH}]_2)\text{Cl}(\text{CO})(\text{PPh}_3)_2$ (**2b**). The IR spectrum for **2a** shows $\nu(\text{CO})$ at 1926, 1911 cm^{-1} , and the corresponding absorptions for **2b** occur at the lower values of 1914, 1899 cm^{-1} . As expected, replacement of Cl on silicon by OH, lowers $\nu(\text{CO})$ [3]. Significantly, $\nu(\text{OH})$ is observed at 3649 cm^{-1} for **1a** and at 3634 cm^{-1} for **1b** and in the ^1H NMR resonances for the silicon-bound OH groups are observed at δ , 2.71 and 2.27 ppm, respectively.

Similarly, treatment of the dichloro(methyl)silyl complexes, **1a** and **1b**, with ethanol/dichloromethane leads rapidly to the formation of the yellow diethoxy (methyl)silyl complexes, $\text{Ru}(\text{SiMe}[\text{OEt}]_2)\text{Cl}(\text{CO})(\text{PPh}_3)_2$ (**3a**) and $\text{Os}(\text{SiMe}[\text{OEt}]_2)\text{Cl}(\text{CO})(\text{PPh}_3)_2$ (**3b**). The IR spectrum for **3a** shows $\nu(\text{CO})$ at 1918 cm^{-1} and for **3b** the corresponding band is at 1904 cm^{-1} . The crystal structure of **3b** was determined. Crystal data and refinement details for **3b**, and for all other structures reported in this paper, are given in Table 1. The molecular structure of **3b** is shown in Fig. 1 and selected bond lengths and angles are given in Table 2. As expected, the geometry about osmium is pyramidal with the silyl ligand in the apical site. This same geometry has been found for other five-coordinate silyl complexes of osmium(II) [2,3,5,16,17]. The Os–Si distance in **3b** is $2.3196(11)\text{ \AA}$, which is very close to the corresponding values found for $\text{Os}[\text{Si}(\text{OH})_3]\text{Cl}(\text{CO})(\text{PPh}_3)_2$ ($2.319(2)\text{ \AA}$) [3] and $\text{Os}[\text{Si}(\text{OEt})_3]\text{Cl}(\text{CO})(\text{PPh}_3)_2$ ($2.319(2)\text{ \AA}$) [16]. A comparison with the Os–Si distance in the six-coordinate dicarbonyl derivative of **3b** will be made in the following section.

2.2. Carbonylation of $\text{Os}[\text{SiMe}(\text{OEt})_2]\text{Cl}(\text{CO})(\text{PPh}_3)_2$ (**3b**) to give $\text{Os}[\text{SiMe}(\text{OEt})_2]\text{Cl}(\text{CO})_2(\text{PPh}_3)_2$ (**4b**), and a comparison of the crystal structures of **3b** and **4b**

As shown in Scheme 1, **3b** reacts with CO to form the colourless, six-coordinate dicarbonyl complex, $\text{Os}[\text{Si}$

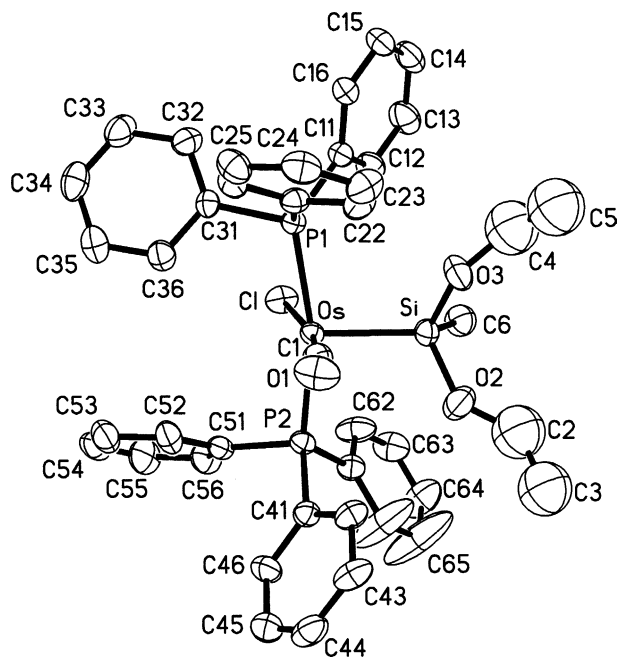


Fig. 1. Molecular geometry of $\text{Os}(\text{SiMe}[\text{OEt}]_2)\text{Cl}(\text{CO})(\text{PPh}_3)_2$ (**3b**).

$\text{Me}(\text{OEt})_2]\text{Cl}(\text{CO})_2(\text{PPh}_3)_2$ (**4b**). The IR spectrum of **4b** has two $\nu(\text{CO})$ bands at $2018, 1959\text{ cm}^{-1}$ consistent with a *cis* arrangement of the two CO ligands. The ^{13}C NMR spectrum, which is also consistent with this arrangement, shows two down-field signals for the different

Table 1
Data collection and processing parameters for **3b**, **4b**, **5a**, **6c**, and **7b**

| | 3b | 4b | 5a ·1/2(C ₆ H ₆) | 6c | 7b |
|---|--|--|---|---|---|
| Formula | C ₄₂ H ₄₃ ClO ₃ OsP ₂ Si | C ₄₃ H ₄₃ ClO ₄ OsP ₂ Si | C ₃₂ H ₂₉ Cl ₃ N ₂ OPRuSi | C ₃₁ H ₂₉ Cl ₂ N ₂ O ₂ PRuSi | C ₃₀ H ₂₈ ClN ₄ OOsPSi |
| Molecular weight | 911.44 | 939.45 | 724.05 | 692.59 | 745.27 |
| Crystal system | Triclinic | Triclinic | Triclinic | Monoclinic | Monoclinic |
| Space group | <i>P</i> $\bar{1}$ | <i>P</i> $\bar{1}$ | <i>P</i> $\bar{1}$ | <i>P</i> ₂ / <i>n</i> | <i>P</i> ₂ / <i>n</i> |
| <i>a</i> (Å) | 10.3486(1) | 10.5619(2) | 10.7815(2) | 9.6362(1) | 11.8140(1) |
| <i>b</i> (Å) | 12.0345(1) | 12.6233(2) | 10.9433(2) | 16.2133(2) | 16.1187(1) |
| <i>c</i> (Å) | 17.3899(1) | 15.9928(2) | 15.3693(3) | 20.6404(3) | 17.2170(1) |
| α (°) | 72.621(1) | 73.358(1) | 99.920(1) | 90.0 | 90.0 |
| β (°) | 89.010(1) | 89.529(1) | 99.910(1) | 103.221(1) | 102.075(1) |
| γ (°) | 72.624(1) | 83.332(1) | 109.72(1) | 90.0 | 90.0 |
| <i>V</i> (Å ³) | 1966.38(3) | 2028.42(6) | 1628.79(5) | 3139.27(7) | 3205.9(3) |
| <i>Z</i> | 2 | 2 | 2 | 4 | 4 |
| <i>D</i> _(calc) (g cm ⁻³) | 1.539 | 1.817 | 1.476 | 1.465 | 1.544 |
| <i>F</i> ₍₀₀₀₎ | 912 | 1114 | 734 | 1408 | 1548 |
| μ (mm ⁻¹) | 3.46 | 3.37 | 0.84 | 0.79 | 4.26 |
| Crystal size (mm) | 0.42×0.35×0.18 | 0.28×0.08×0.06 | 0.42×0.22×0.12 | 0.44×0.14×0.12 | 0.12×0.12×0.08 |
| 2 θ (min–max) (°) | 1.2–27.2 | 1.3–26.3 | 1.4–27.1 | 1.6–27.1 | 1.7–27.1 |
| Reflections collected | 19,651 | 18,946 | 16,035 | 30,451 | 19,314 |
| Independent reflections (<i>R</i> _{int}) | 8519 (0.0218) | 8051 (0.0230) | 6965 (0.0195) | 6773 (0.0493) | 6913 (0.0337) |
| <i>A</i> (min–max) | 0.324–0.575 | 0.452–0.823 | 0.719–0.906 | 0.723–0.911 | 0.634–0.731 |
| Goodness-of-fit on <i>F</i> ² | 1.044 | 1.085 | 1.065 | 1.169 | 1.047 |
| <i>R</i> (observed data) | <i>R</i> ₁ = 0.0339 <i>wR</i> ₂ = 0.0857 | <i>R</i> ₁ = 0.0236 <i>wR</i> ₂ = 0.0517 | <i>R</i> ₁ = 0.0371 <i>wR</i> ₂ = 0.1069 | <i>R</i> ₁ = 0.0621 <i>wR</i> ₂ = 0.1506 | <i>R</i> ₁ = 0.0312 <i>wR</i> ₂ = 0.0581 |
| <i>R</i> (all data) | <i>R</i> ₁ = 0.0352 <i>wR</i> ₂ = 0.0866 | <i>R</i> ₁ = 0.0285 <i>wR</i> ₂ = 0.0542 | <i>R</i> ₁ = 0.0418 <i>wR</i> ₂ = 0.1128 | <i>R</i> ₁ = 0.0712 <i>wR</i> ₂ = 0.1554 | <i>R</i> ₁ = 0.0466 <i>wR</i> ₂ = 0.0628 |
| Diff. map (min–max) (e [−] Å ^{−3}) | 1.81–1.22 | 0.87–0.75 | 1.82–0.85 | 1.72–1.35 | 0.78–0.57 |

$$R = \frac{\sum ||F_o| - |F_c||}{\sum |F_o|}$$

$$wR_2 = \frac{\sum \{[w(F_o^2 - F_c^2)]^2\}}{\sum [w(F_o^2)]^2}^{1/2}$$

Table 2
Selected bond lengths (Å) and angles (°) for **3b**

| Bond lengths | |
|--------------|------------|
| Os–C(1) | 1.824(5) |
| Os–Si | 2.3196(11) |
| Os–P(1) | 2.3617(10) |
| Os–P(2) | 2.3671(10) |
| Os–Cl | 2.4039(11) |
| Si–O(3) | 1.639(4) |
| Si–O(2) | 1.651(4) |
| Si–C(6) | 1.879(5) |
| O(1)–C(1) | 1.139(6) |
| Bond angles | |
| C(1)–Os–Si | 84.87(16) |
| C(1)–Os–P(1) | 88.77(14) |
| Si–Os–P(1) | 98.05(4) |
| C(1)–Os–P(2) | 93.09(14) |
| Si–Os–P(2) | 95.94(4) |
| P(1)–Os–P(2) | 165.99(4) |
| C(1)–Os–Cl | 167.38(16) |
| Si–Os–Cl | 107.42(4) |
| P(1)–Os–Cl | 86.73(4) |
| P(2)–Os–Cl | 88.52(4) |
| O(3)–Si–O(2) | 104.9(2) |
| O(3)–Si–C(6) | 107.2(2) |
| O(2)–Si–C(6) | 106.9(2) |
| O(3)–Si–Os | 111.85(13) |
| O(2)–Si–Os | 112.29(14) |
| C(6)–Si–Os | 113.16(18) |

CO ligands at 177.4 and 180.4 ppm. This geometry is confirmed by a crystal structure determination. The molecular structure of **4b** is shown in Fig. 2 and selected bond lengths and angles are given in Table 3. The geometry about osmium is octahedral with mutually *trans* triphenylphosphine ligands and mutually *cis* CO ligands. The most interesting structural parameter is the Os–Si

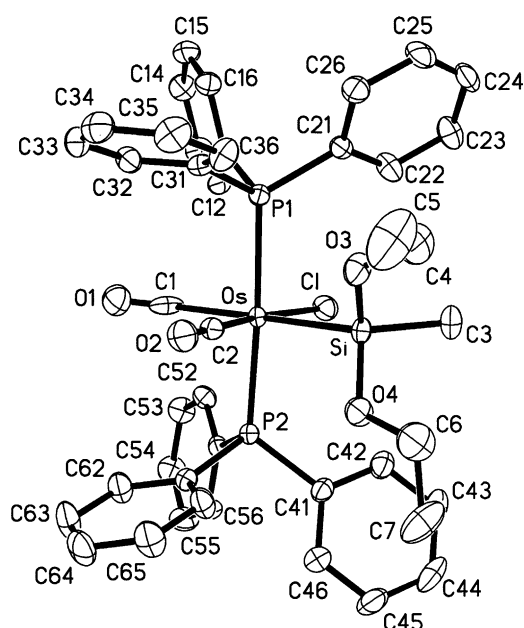


Fig. 2. Molecular geometry of Os(SiMe[OEt]₂)Cl(CO)₂(PPh₃)₂ (**4b**).

Table 3
Selected bond lengths (Å) and angles (°) for **4b**

| Bond lengths | |
|--------------|------------|
| Os–C(2) | 1.887(3) |
| Os–C(1) | 2.024(4) |
| Os–P(2) | 2.4084(8) |
| Os–P(1) | 2.4149(8) |
| Os–Cl | 2.4837(8) |
| Os–Si | 2.4901(8) |
| Si–O(3) | 1.672(2) |
| Si–O(4) | 1.676(2) |
| Si–C(3) | 1.892(3) |
| O(1)–C(1) | 1.049(4) |
| O(2)–C(2) | 1.149(4) |
| Bond angles | |
| C(2)–Os–C(1) | 87.69(13) |
| C(2)–Os–P(2) | 93.22(9) |
| C(1)–Os–P(2) | 87.65(9) |
| C(2)–Os–P(1) | 91.11(9) |
| C(1)–Os–P(1) | 86.89(9) |
| P(2)–Os–P(1) | 172.89(3) |
| C(2)–Os–Cl | 172.22(9) |
| C(1)–Os–Cl | 99.96(10) |
| P(2)–Os–Cl | 85.72(3) |
| P(1)–Os–Cl | 90.74(3) |
| C(2)–Os–Si | 79.86(10) |
| C(1)–Os–Si | 167.38(9) |
| P(2)–Os–Si | 95.03(3) |
| P(1)–Os–Si | 91.28(3) |
| Cl–Os–Si | 92.54(3) |
| O(3)–Si–O(4) | 107.71(13) |
| O(3)–Si–C(3) | 105.81(15) |
| O(4)–Si–C(3) | 105.59(15) |
| O(3)–Si–Os | 106.91(9) |
| O(4)–Si–Os | 108.20(9) |
| C(3)–Si–Os | 121.94(11) |

bond distance which is 2.4901(8) Å. This is an increase of 0.1705 Å over the corresponding distance found in the five-coordinate complex **3b**. Almost identical increases were observed for the related pairs of osmium(II)-silyl complexes Os[Si(OEt)₃]R(CO)(PPh₃)₂ and Os[Si(OEt)₃]R(CO)₂(PPh₃)₂ (an increase of 0.1688 Å (for R = Ph), and an increase of 0.1546 Å (for R = *o*-tolyl)) [16]. All the other Os–ligand bond distances in **4b** are also increased with respect to the values found in **3b** but the increases are much smaller. It should also be noted that the CO ligand *trans* to the silyl ligand is bound at a distance of 2.024(4) Å whereas the other CO is bound at 1.887(3) Å. Clearly, the silyl and CO ligands, when located mutually *trans*, have a pronounced bond lengthening effect on each other.

2.3. Reaction of *M*(SiMeCl₂)Cl(CO)(PPh₃)₂ (**1a**, *M* = Ru; **1b**, *M* = Os) with 8-aminoquinoline to give *M*(SiMeCl₂)Cl(CO)(PPh₃)(κ²(*N,N*)-NC₉H₆NH₂-8) (**5a**, *M* = Ru; **5b**, *M* = Os) and the crystal structure of **5a**

In view of the reactivity of **1a** and **1b** towards the OH functions in water and ethanol discussed in Section 2.1,

it was of interest to explore the corresponding reactivity towards NH functions in appropriate molecules. Our experience with the nucleophilic substitution reactions of the BCl_2 ligand bound to osmium in $\text{Os}(\text{BCl}_2)\text{Cl}(\text{CO})(\text{PPh}_3)_2$ showed that more tractable derivatives were obtained in reactions with molecules which had not only NH functions but also a separate donor function so that the resulting amino-boryl ligands became tethered to the osmium [19–21]. Accordingly, the reactions of **1a** and **1b** with 8-aminoquinoline and 2-aminopyridine (discussed in Section 2.4) were examined. As shown in Scheme 2, treatment of either **1a** or **1b** with one equivalent of 8-aminoquinoline, even in the presence of excess triethylamine, gave the coordinatively saturated, orange compounds, $\text{Ru}(\text{SiMeCl}_2)\text{Cl}(\text{CO})(\text{PPh}_3)(\kappa^2(N,N)\text{-NC}_9\text{H}_6\text{NH}_2\text{-8})$ (**5a**) or $\text{Os}(\text{SiMeCl}_2)\text{Cl}(\text{CO})(\text{PPh}_3)(\kappa^2(N,N)\text{-NC}_9\text{H}_6\text{NH}_2\text{-8})$ (**5b**), respectively. Surprisingly, no condensation of the Si–Cl bonds with the 8-aminoquinoline N–H bonds occurred. Rather, the 8-aminoquinoline coordinated unchanged as a bidentate ligand through the two nitrogen atoms with displacement of a triphenylphosphine ligand. The IR spectra of **5a** and **5b** show a single $\nu(\text{CO})$ at 1944 and 1892 cm^{-1} , respectively. The ^1H NMR spectra show two doublet signals for the NH_2 protons at 3.99 ppm ($^2J_{\text{HH}}=12$ Hz), 4.44 ppm ($^2J_{\text{HH}}=12$ Hz) (**5a**) and 3.95 ppm ($^2J_{\text{HH}}=11.6$ Hz), 4.82 ppm ($^2J_{\text{HH}}=12.4$ Hz) (**5b**), respectively. This is consistent with there being two proton environments for the NH_2 donor group, as can be seen in the structure depicted in Scheme 2. This structure was confirmed by crystal structure analysis of $\text{Ru}(\text{SiMeCl}_2)\text{Cl}(\text{CO})(\text{PPh}_3)(\kappa^2(N,N)\text{-NC}_9\text{H}_6\text{NH}_2\text{-8})$ (**5a**). The molecular geometry of **5a** is shown in Fig. 3 and

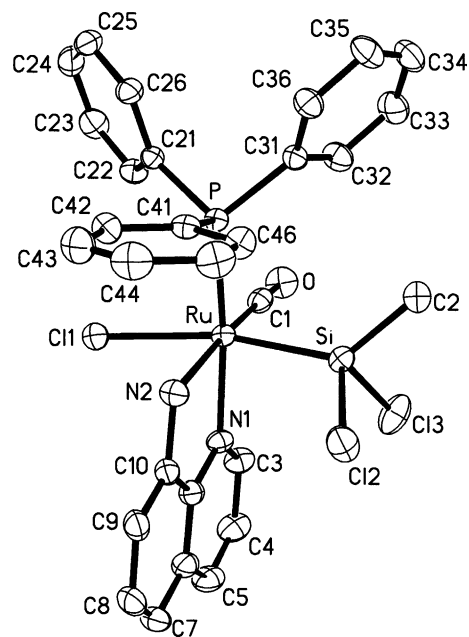
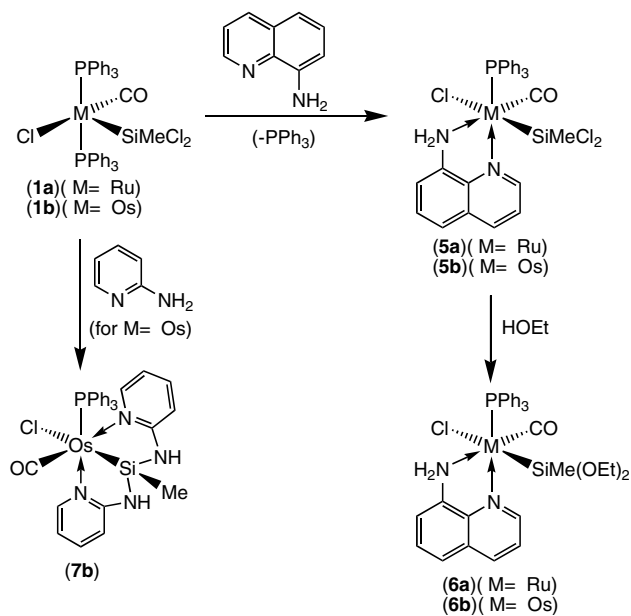


Fig. 3. Molecular geometry of $\text{Ru}(\text{SiMeCl}_2)\text{Cl}(\text{CO})(\text{PPh}_3)(\kappa^2(N,N)\text{-NC}_9\text{H}_6\text{NH}_2\text{-8})$ (**5a**).

selected bond lengths and angles are given in Table 4. The geometry about ruthenium is octahedral with the 8-aminoquinoline coordinated as a bidentate ligand. The quinoline nitrogen is *trans* to triphenylphosphine and the amino nitrogen is *trans* to carbonyl. It should be noted that this arrangement leaves the Si–Cl bonds adjacent to the coordinated NH_2 function, yet remarkably, as noted above no condensation occurs. The Ru–Si distance is 2.3389(8) Å while the Ru–Cl distance is 2.5164(7) Å indicating the powerful *trans* influence of the silyl ligand. The bidentate 8-aminoquinoline is bound with the Ru–N(quinoline) distance at 2.119(2) Å and the Ru– NH_2 distance at 2.193(2) Å. The two Si–Cl distances are almost identical at 2.1210(11) and 2.1247(11) Å.

Despite the lack of reactivity of the Si–Cl bonds in **5a** and **5b** towards the N–H functions in the coordinated 8-aminoquinoline, both **5a** and **5b** react readily with ethanol to give ultimately the diethoxymethylsilyl products, $\text{Ru}[\text{SiMe}(\text{OEt})_2]\text{Cl}(\text{CO})(\text{PPh}_3)(\kappa^2(N,N)\text{-NC}_9\text{H}_6\text{NH}_2\text{-8})$ (**6a**) and $\text{Os}[\text{SiMe}(\text{OEt})_2]\text{Cl}(\text{CO})(\text{PPh}_3)(\kappa^2(N,N)\text{-NC}_9\text{H}_6\text{NH}_2\text{-8})$ (**6b**), respectively (see Scheme 2). The IR spectrum of **6a** shows a single $\nu(\text{CO})$ at 1907 cm^{-1} and the corresponding band for **6b** is at 1894 cm^{-1} . The presence of two diastereotopic ethoxy groups, as required by the structure, is shown by NMR spectroscopy. The ^{13}C NMR spectra show doublet signals for the carbonyl ligands at 205.8 ppm ($^2J_{\text{CP}}=28.2$ Hz) for **6a** and at 189.5 ppm ($^2J_{\text{CP}}=12.1$ Hz) for **6b**.

During efforts to grow crystals of **5a** suitable for X-ray structure analysis from $\text{CH}_2\text{Cl}_2/\text{EtOH}$ solution a single crystal of the product of partial ethanolysis of **5a**, i.e., $\text{Ru}[\text{SiMeCl}(\text{OEt})]\text{Cl}(\text{CO})(\text{PPh}_3)(\kappa^2(N,N)\text{-NC}_9\text{H}_6\text{-NH}_2\text{-8})$



Scheme 2. Reactions of dichloro(methyl)silyl complexes of ruthenium(II) and osmium(II) with 8-aminoquinoline and 2-aminopyridine.

Table 4
Selected bond lengths (Å) and angles (°) for **5a**

| Bond lengths | |
|----------------|------------|
| Ru–C(1) | 1.841(3) |
| Ru–N(1) | 2.119(2) |
| Ru–N(2) | 2.193(2) |
| Ru–P | 2.3183(7) |
| Ru–Si | 2.3389(8) |
| Ru–Cl(1) | 2.5164(7) |
| Si–C(2) | 1.857(3) |
| Si–Cl(3) | 2.1210(11) |
| Si–Cl(2) | 2.1247(11) |
| O–C(1) | 1.146(4) |
| Bond angles | |
| C(1)–Ru–N(1) | 95.35(11) |
| C(1)–Ru–N(2) | 173.73(11) |
| N(1)–Ru–N(2) | 78.43(9) |
| C(1)–Ru–P | 91.67(9) |
| N(1)–Ru–P | 172.56(7) |
| N(2)–Ru–P | 94.51(7) |
| C(1)–Ru–Si | 88.29(9) |
| N(1)–Ru–Si | 87.44(7) |
| N(2)–Ru–Si | 92.17(7) |
| P–Ru–Si | 95.26(3) |
| C(1)–Ru–Cl(1) | 100.07(9) |
| N(1)–Ru–Cl(1) | 83.28(7) |
| N(2)–Ru–Cl(1) | 78.59(7) |
| P–Ru–Cl(1) | 93.07(3) |
| Si–Ru–Cl(1) | 168.02(3) |
| C(2)–Si–Cl(3) | 100.15(13) |
| C(2)–Si–Cl(2) | 101.10(13) |
| Cl(3)–Si–Cl(2) | 99.93(5) |
| C(2)–Si–Ru | 131.31(12) |
| Cl(3)–Si–Ru | 110.88(4) |
| Cl(2)–Si–Ru | 109.01(4) |

(**6c**), was inadvertently obtained. A bulk sample of **6c** as a pure compound was not obtained, however, the opportunity to complete the crystal structure was taken. The molecular geometry of **6c** is shown in Fig. 4 and selected bond lengths and angles are given in Table 5. The arrangement of the six donor atoms about ruthenium is exactly the same as for **5a** discussed above. The effect of replacing one chloride on silicon with an ethoxy group is to lengthen both the Ru–Si bond (from 2.3389(8) Å in **5a** to 2.3486(15) Å in **6c**) and the Ru–Cl bond (from 2.5164(7) Å in **5a** to 2.5633(13) Å in **6c**). Clearly the *trans* influence of the silyl ligand is strongly increased by this substitution of chloride by ethoxide. Other molecular parameters for **6c** are substantially unchanged from those for **5a**.

2.4. Reaction of *Os*(SiMeCl₂)Cl(CO)(PPh₃)₂ (**1b**) with 2-aminopyridine to give *Os*(κ³(Si,N,N)-SiMe[NH(2-C₅H₄N)]₂)Cl(CO)(PPh₃) (**7b**), and the crystal structure of **7b**

Whereas the reaction of **1b** with 8-aminoquinoline described above resulted in coordination of 8-aminoquinoline as a bidentate ligand and left the dichloromethylsilyl

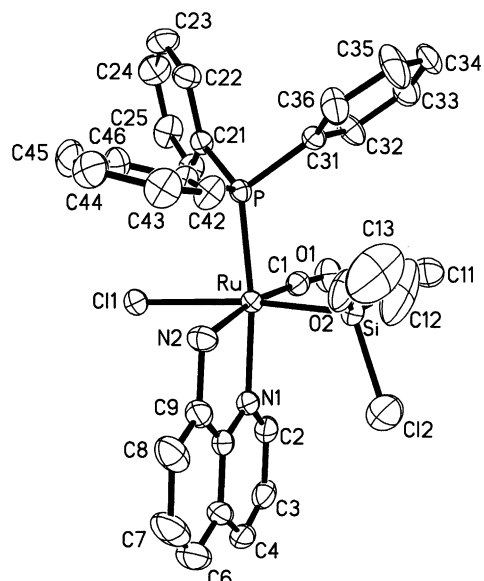


Fig. 4. Molecular geometry of Ru(SiMeCl(OEt))Cl(CO)(PPh₃)-(κ²(N,N)-NC₉H₆NH₂-8) (**6c**).

Table 5
Selected bond lengths (Å) and angles (°) for **6c**

| Bond lengths | |
|----------------|------------|
| Ru–C(1) | 1.821(6) |
| Ru–N(1) | 2.132(4) |
| Ru–N(2) | 2.204(5) |
| Ru–P | 2.3195(13) |
| Ru–Si | 2.3486(15) |
| Ru–Cl(1) | 2.5633(13) |
| Si–O(2) | 1.663(5) |
| Si–C(11) | 1.837(7) |
| Si–Cl(2) | 2.086(2) |
| O(1)–C(1) | 1.172(7) |
| Bond angles | |
| C(1)–Ru–N(1) | 95.1(2) |
| C(1)–Ru–N(2) | 170.8(2) |
| N(1)–Ru–N(2) | 78.65(18) |
| C(1)–Ru–P | 92.57(16) |
| N(1)–Ru–P | 171.23(13) |
| N(2)–Ru–P | 94.18(12) |
| C(1)–Ru–Si | 86.91(16) |
| N(1)–Ru–Si | 91.41(12) |
| N(2)–Ru–Si | 86.45(13) |
| P–Ru–Si | 93.20(5) |
| C(1)–Ru–Cl(1) | 106.00(16) |
| N(1)–Ru–Cl(1) | 84.76(12) |
| N(2)–Ru–Cl(1) | 80.40(13) |
| P–Ru–Cl(1) | 89.09(4) |
| Si–Ru–Cl(1) | 166.79(5) |
| O(2)–Si–C(11) | 108.6(3) |
| O(2)–Si–Cl(2) | 103.3(2) |
| C(11)–Si–Cl(2) | 100.9(2) |
| O(2)–Si–Ru | 107.49(16) |
| C(11)–Si–Ru | 122.4(2) |
| Cl(2)–Si–Ru | 112.54(9) |
| C(12)–O(2)–Si | 123.6(5) |

ligand unchanged, the reaction of **1b** with two equivalents of 2-aminopyridine leads to condensation of the amino N–H functions with both Si–Cl bonds forming a novel tridentate silyl ligand in the complex $\text{Os}(\kappa^3(\text{Si}, \text{N}, \text{N})\text{-SiMe}[\text{NH}(2\text{-C}_5\text{H}_4\text{N})]_2)\text{Cl}(\text{CO})(\text{PPh}_3)$ (**7b**) (see Scheme 2). This marked difference in behaviour between 8-aminoquinoline and 2-aminopyridine can be attributed to the formation of favourable five-membered rings in the structure of **7b** (the analogous reaction with 8-aminoquinoline would produce less-favourable six-membered rings). In a closely related reaction the chlorodimethylsilyl ligand in $\text{CpFe}(\text{CO})_2(\text{SiClMe}_2)$ has been treated with the sodium salt of 2-hydroxypyridine to give $\text{CpFe}(\text{CO})_2[\text{SiMe}_2\text{O}(2\text{-C}_5\text{H}_4\text{N})]$ and this compound in turn when subjected to photolysis loses CO and forms the bidentate chelate complex, $\text{CpFe}(\text{CO})[\kappa^2(\text{Si}, \text{N})\text{-SiMe}_2\text{O}(2\text{-C}_5\text{H}_4\text{N})]$ [22]. A compound with a tridentate ligand related to the ligand found in **7b** in that it is a “NSiN” donor has been reported from an oxidative addition reaction utilizing a preformed bis(8-quinolyl)silane [23]. The IR spectrum of pale yellow **7b** has $\nu(\text{CO})$ at 1900 cm^{-1} . The ^1H NMR spectrum of **7b** shows singlet signals for the two different NH groups at 4.95 and 5.18 ppm. In the ^{13}C NMR the carbonyl carbon resonance is a doublet at 186.8 ppm ($^2J_{\text{CP}} = 12.1\text{ Hz}$). To confirm the presence of a tridentate ligand and to ascertain the geometry of attachment to osmium the crystal structure of **7b** was determined. The molecular geometry is shown in Fig. 5 and selected bond lengths and angles are given in Table 6. The Os–Si distance is 2.3121(12) Å which is very short for an octahedral osmium silyl complex and is very close to the Os–Si distance found in the five-coordinate complex **3b** (2.3196(11) Å). The two Os–N distances are not equal (2.176(4) Å for N *trans* to

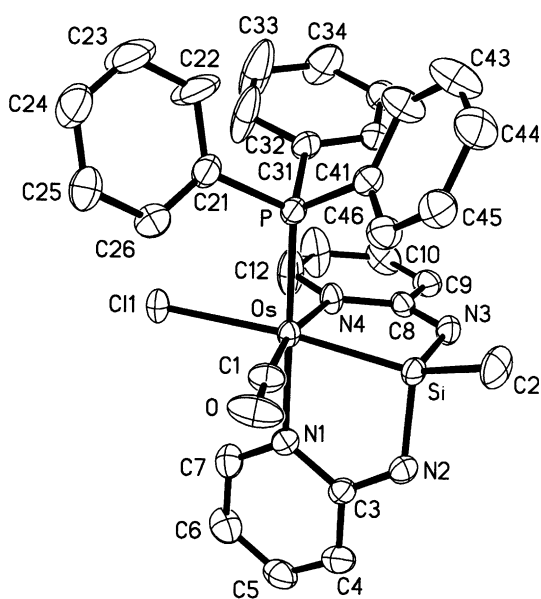


Fig. 5. Molecular geometry of $\text{Os}(\kappa^3(\text{Si}, \text{N}, \text{N})\text{-SiMe}[\text{NH}(2\text{-C}_5\text{H}_4\text{N})]_2)\text{Cl}(\text{CO})(\text{PPh}_3)$ (**7b**).

Table 6
Selected bond lengths (Å) and angles (°) for **7b**

| Bond lengths | |
|---------------|------------|
| Os–C(1) | 1.829(5) |
| Os–N(1) | 2.176(4) |
| Os–N(4) | 2.198(4) |
| Os–P | 2.3085(12) |
| Os–Si | 2.3121(12) |
| Os–Cl(1) | 2.5503(11) |
| Si–N(3) | 1.767(4) |
| Si–N(2) | 1.777(4) |
| Si–C(2) | 1.863(5) |
| O–C(1) | 1.177(6) |
| Bond angles | |
| C(1)–Os–N(1) | 91.0(2) |
| C(1)–Os–N(4) | 169.1(2) |
| N(1)–Os–N(4) | 84.0(1) |
| C(1)–Os–P | 92.7(2) |
| N(1)–Os–P | 176.3(1) |
| N(4)–Os–P | 92.5(1) |
| C(1)–Os–Si | 89.2(2) |
| N(1)–Os–Si | 79.8(1) |
| N(4)–Os–Si | 80.4(1) |
| P–Os–Si | 101.06(4) |
| C(1)–Os–Cl(1) | 98.7(2) |
| N(1)–Os–Cl(1) | 90.9(1) |
| N(4)–Os–Cl(1) | 91.1(1) |
| P–Os–Cl(1) | 87.68(4) |
| Si–Os–Cl(1) | 168.00(4) |
| N(3)–Si–N(2) | 107.8(2) |
| N(3)–Si–C(2) | 105.3(2) |
| N(2)–Si–C(2) | 103.4(2) |
| N(3)–Si–Os | 100.7(1) |
| N(2)–Si–Os | 99.8(1) |
| C(2)–Si–Os | 137.5(2) |

PPh_3 , and 2.198(4) for N *trans* to CO). The chloride, which is located *trans* to the Si donor, is attached at the very long distance of 2.5503(11) Å. The two Si–N distances (1.767(4) and 1.777(4) Å) are at the long end of the range observed for normal Si–N single bonds (1.70–1.76 Å).

3. Conclusions

It has been demonstrated that the dichloro(methyl)silyl ligand in the five-coordinate complexes of ruthenium and osmium, $\text{M}(\text{SiCl}_2\text{Me})\text{Cl}(\text{CO})(\text{PPh}_3)_2$, readily undergoes condensation reactions with either the O–H function in water and ethanol or the N–H function in 2-aminopyridine giving hydroxysilyl, ethoxysilyl, or 2-pyridylaminosilyl complexes, respectively. The last reaction gives rise to a tridentate “NSiN” ligand indicating how novel multi-dentate silyl ligands might be assembled through nucleophilic substitution reactions of the Si–Cl bonds of chlorosilyl ligands. In contrast to the facility with which 2-aminopyridine reacts with $\text{M}(\text{SiCl}_2\text{Me})\text{Cl}(\text{CO})(\text{PPh}_3)_2$, 8-aminoquinoline coordinates unchanged,

with triphenylphosphine displacement. This difference in the reactivity of Si–Cl bonds has been attributed to the formation of favourable five-membered rings in the reaction with 2-aminopyridine whereas any analogous reaction with 8-aminoquinoline would form six-membered rings. The structures of key compounds have been determined by X-ray crystallography confirming that short M–Si distances depend not only on the presence of electronegative substituents on Si but also on whether the metal is five- or six-coordinate and whether the Si is part of a chelate ring system.

4. Experimental

4.1. General procedures and instruments

Standard laboratory procedures were followed as have been described previously [13]. The compounds $\text{RuHCl}(\text{CO})(\text{PPh}_3)_3$ [24], $\text{RuPhCl}(\text{CO})(\text{PPh}_3)_2$ [25] and $\text{OsPhCl}(\text{CO})(\text{PPh}_3)_2$ [25], were prepared by literature methods.

Infrared spectra ($4000\text{--}400\text{ cm}^{-1}$) were recorded as Nujol mulls between KBr plates on a Perkin–Elmer Paragon 1000 spectrometer. NMR spectra were obtained on either a Bruker DRX 400 or Bruker AC 200 at $25\text{ }^\circ\text{C}$. For the Bruker DRX 400, ^1H and ^{13}C NMR spectra were obtained operating at 400.1 (^1H) and 100.6 (^{13}C) MHz, respectively. For the Bruker AC 200, ^1H and ^{13}C NMR spectra were obtained operating at 200.0 (^1H) and 50.3 (^{13}C) MHz, respectively. Resonances are quoted in ppm and ^1H NMR spectra referenced to either tetramethylsilane (0.00 ppm) or the proteo-impurity in the solvent (7.25 ppm for CHCl_3). ^{13}C NMR spectra were referenced to CDCl_3 (77.00 ppm). Elemental analyses were obtained from the Microanalytical Laboratory, University of Otago.

4.2. Preparation of $\text{Ru}(\text{SiMeCl}_2)\text{Cl}(\text{CO})(\text{PPh}_3)_2$ (**1a**)

To $\text{RuHCl}(\text{CO})(\text{PPh}_3)_3$ (1.08 g, 1.13 mmol) in dry toluene (20 mL) in a Schlenk tube, was added HSiMeCl_2 (2.60 g, 22.6 mmol). The tube was sealed, cooled in liquid nitrogen and then evacuated. After warming to ambient temperature, the sealed tube was shielded with a safety shield (CAUTION: pressure increases as reaction proceeds) and heated in an oil bath at $60\text{ }^\circ\text{C}$ for 1.5 h. Reduction of the volume of the solution in vacuo followed by slow addition of dry hexane afforded pure, yellow crystals of $\text{Ru}(\text{SiMeCl}_2)\text{Cl}(\text{CO})(\text{PPh}_3)_2$, (863 mg, 95%), m.p. $230\text{ }^\circ\text{C}$ (dec.). Anal. Calc. for $\text{C}_{38}\text{H}_{33}\text{Cl}_3\text{OP}_2\text{SiRu}$: C, 56.83 ; H, 4.14 ; Cl, 13.24 . Found: C, 56.99 ; H, 4.19 ; Cl, 13.52% . IR (cm^{-1}): 1923 , 1936 , 1953 $\nu(\text{CO})$. ^1H NMR (CDCl_3 , δ): 0.80 (s, 3H , SiCH_3), $7.38\text{--}7.65$ (m, 30H , PPh_3). ^{13}C NMR (CDCl_3 , δ): 19.2 (s, SiCH_3), 128.4 (t' [13], $^{2,4}J_{\text{CP}}=9.0$ Hz, $o\text{-C}_6\text{H}_5$), 130.5 (s,

$p\text{-C}_6\text{H}_5$), 131.1 (t' , $^{1,3}J_{\text{CP}}=45.2$ Hz, $i\text{-C}_6\text{H}_5$), 134.6 (t' , $^{3,5}J_{\text{CP}}=11.0$ Hz, $m\text{-C}_6\text{H}_5$), 198.3 (t , $^2J_{\text{CP}}=12.6$ Hz, CO).

An alternative preparative method for **1a** is the following: $\text{RuPhCl}(\text{CO})(\text{PPh}_3)_2$ (0.50 g, 0.65 mmol) was dried in vacuo in a Schlenk tube, and benzene (25 mL) was added, and the solvent was degassed. Methylchlorosilane (0.75 g, 6.5 mmol) was then transferred to the reaction vessel by “vacuum freeze trapping” and the tube was sealed. While still under vacuum the mixture was warmed to room temperature and the red suspension was then heated (CAUTION: use safety shield) for 1.5 h in an oil bath maintained at a temperature of $50\text{ }^\circ\text{C}$. After this time a yellow solution was obtained. The solvent volume was reduced in vacuo and hexane (15 mL) was added resulting in the formation of pure **1a** as bright yellow crystals which were then collected by filtration (420 mg, 80%).

4.3. Preparation of $\text{Os}(\text{SiMeCl}_2)\text{Cl}(\text{CO})(\text{PPh}_3)_2$ (**1b**)

$\text{OsPhCl}(\text{CO})(\text{PPh}_3)_2$ (0.43 g, 0.51 mmol) was dried in vacuo in a Schlenk tube, benzene (15 mL) was added and the solution was degassed. Methylchlorosilane (0.587 g, 5.1 mmol) was transferred in a similar manner to that described in Section 4.2. The evacuated Schlenk tube was then heated at $70\text{ }^\circ\text{C}$ with stirring for 15 min (CAUTION: safety shield). The solvent volume was reduced and hexane (15 mL) was added resulting in the formation of a yellow-orange solid which was then collected by filtration. Recrystallization of the solid was carried out in dry benzene and hexane to give pure **1b** as yellow-orange crystals (421 mg, 93%), m.p. $240\text{ }^\circ\text{C}$ (dec.). Anal. Calc. for $\text{C}_{38}\text{H}_{33}\text{Cl}_3\text{OOSiP}_2\text{Os}$: C, 51.15 ; H, 3.73 ; Cl, 11.92 . Found: C, 51.29 ; H, 3.86 ; Cl, 11.97% . IR (cm^{-1}): 1911 , 1925 , 1942 $\nu(\text{CO})$. ^1H NMR (CDCl_3 , δ): 0.69 (s, 3H , SiCH_3), $7.36\text{--}7.74$ (m, 30H , PPh_3). ^{13}C NMR (CDCl_3 , δ): 17.1 (s, SiCH_3), 128.3 (t' , $^{2,4}J_{\text{CP}}=9.0$ Hz, $o\text{-C}_6\text{H}_5$), 130.6 (s, $p\text{-C}_6\text{H}_5$), 130.8 (t' , $^{1,3}J_{\text{CP}}=52.2$ Hz, $i\text{-C}_6\text{H}_5$), 134.8 (t' , $^{3,5}J_{\text{CP}}=11.0$ Hz, $m\text{-C}_6\text{H}_5$), 181.0 (t , $^2J_{\text{CP}}=8.6$ Hz, CO).

4.4. Preparation of $\text{Ru}(\text{SiMe}[\text{OH}]_2)\text{Cl}(\text{CO})(\text{PPh}_3)_2$ (**2a**)

$\text{Ru}(\text{SiMeCl}_2)\text{Cl}(\text{CO})(\text{PPh}_3)_2$ (0.10 g, 0.12 mmol) was added to a suspension of K_2CO_3 (0.5 g, excess) in degassed THF (10 mL) and water (1 mL). The mixture was stirred for 5 min during which time the yellow solution underwent no visible colour change. The solvent was evaporated to dryness to give a yellow solid and this was redissolved in dichloromethane and filtered to remove the potassium salts. A yellow solid was obtained from this solution by reduction of the solvent volume, followed by the addition of ethanol. Recrystallization was carried out in dichloromethane/hexane to give pure **2a** as a yellow crystalline solid (62 mg, 65%), m.p. $200\text{ }^\circ\text{C}$

(dec.). Anal. Calc. for $C_{38}H_{33}ClO_3P_2RuSi$: C, 59.57; H, 4.60; Cl, 4.63. Found: C, 59.38; H, 4.22; Cl, 4.87%. IR (cm^{-1}): 1911, 1926 $\nu(CO)$; 3649w $\nu(OH)$. 1H NMR ($CDCl_3$, δ): 0.23 (s, 3H, $SiCH_3$), 2.71 (s, 2H, $Si(OH)_2$), 7.36–7.64 (m, 30H, PPh_3). ^{13}C NMR ($CDCl_3$, δ): 8.6 (s, $SiCH_3$), 128.5 (t' , $^{2,4}J_{CP}=9.0$ Hz, $o-C_6H_5$), 130.4 (s, $p-C_6H_5$), 131.9 (t' , $^{1,3}J_{CP}=44.2$ Hz, $i-C_6H_5$), 134.3 (t' , $^{3,5}J_{CP}=12.0$ Hz, $m-C_6H_5$), 199.1 (t , $^2J_{CP}=13.6$ Hz, CO).

4.5. Preparation of $Os(SiMe[OH]_2)Cl(CO)(PPh_3)_2$ (**2b**)

$Os(SiMeCl_2)Cl(CO)(PPh_3)_2$ (0.080 g, 0.090 mmol) was added to a suspension of K_2CO_3 (0.5 g, excess) in degassed THF (10 mL) and water (1 mL). The mixture was stirred for 5 min during which time the yellow solution underwent no visible colour change. The solvent was evaporated to dryness to give an orange solid and this was redissolved in dichloromethane and filtered to remove the potassium salts. An orange solid was obtained from this solution by reduction of the solvent volume, followed by the addition of ethanol. Recrystallization was carried out in dichloromethane/hexane to give pure **2b** as an orange crystalline solid (45 mg, 59%), m.p. 195 °C (dec.). Anal. Calc. for $C_{38}H_{33}ClO_3OsP_2Si$: C, 53.36; H, 4.12. Found: C, 52.96; H, 4.04%. IR (cm^{-1}): 1899, 1914 $\nu(CO)$; 3634w $\nu(OH)$. 1H NMR ($CDCl_3$, δ): 0.17 (s, 3H, $SiCH_3$), 2.27 (s, 2H, $Si(OH)_2$), 7.37–7.65 (m, 30H, PPh_3). ^{13}C NMR ($CDCl_3$, δ): 7.8 (s, $SiCH_3$), 128.4 (t' , $^{2,4}J_{CP}=9.0$ Hz, $o-C_6H_5$), 130.5 (s, $p-C_6H_5$), 131.8 (t' , $^{1,3}J_{CP}=50.4$ Hz, $i-C_6H_5$), 134.5 (t' , $^{3,5}J_{CP}=11.0$ Hz, $m-C_6H_5$), 182.5 (t , $^2J_{CP}=8.6$ Hz, CO).

4.6. Preparation of $Ru(SiMe[OEt]_2)Cl(CO)(PPh_3)_2$ (**3a**)

$Ru(SiMeCl_2)Cl(CO)(PPh_3)_2$ (0.100 g, 0.12 mmol) was dissolved in dichloromethane (10 mL), ethanol (2 mL) was added and the resulting solution was stirred at room temperature for 5 min. The solvent volume was then reduced and hexane was added to precipitate a yellow solid. The yellow product was recrystallized from dichloromethane and hexane to yield yellow crystals of pure **3a** (52 mg, 51%), m.p. 182–184 °C (dec.). Anal. Calc. for $C_{42}H_{43}ClO_3P_2RuSi$: C, 61.34; H, 5.27; Cl, 4.31. Found: C, 60.94; H, 5.26; Cl, 4.55%. IR (cm^{-1}): 1918 $\nu(CO)$. 1H NMR ($CDCl_3$, δ): 0.19 (s, 3H, $SiCH_3$), 0.87 (t , 6H, $^3J_{HH}=7.0$ Hz, $Si(OCH_2CH_3)_2$), 3.38 (q, 4H, $^3J_{HH}=7.0$ Hz, $Si(OCH_2CH_3)_2$), 7.28–7.70 (m, 30H, PPh_3). ^{13}C NMR ($CDCl_3$, δ): 5.4 (s, $SiCH_3$), 17.8 (s, $Si(OCH_2CH_3)_2$), 58.5 (s, $Si(OCH_2CH_3)_2$), 127.9 (t' , $^{2,4}J_{CP}=9.0$ Hz, $o-C_6H_5$), 129.9 (s, $p-C_6H_5$), 133.0 (t' , $^{1,3}J_{CP}=43.2$ Hz, $i-C_6H_5$), 134.7 (t' , $^{3,5}J_{CP}=11.0$ Hz, $m-C_6H_5$), 199.9 (t , $^2J_{CP}=13.6$ Hz, CO).

4.7. Preparation of $Os(SiMe[OEt]_2)Cl(CO)(PPh_3)_2$ (**3b**)

$Os(SiMeCl_2)Cl(CO)(PPh_3)_2$ (0.100 g, 0.11 mmol) was dissolved in dichloromethane (10 mL), ethanol (2 mL) was added and the resulting yellow solution was stirred at room temperature for 5 min. The solvent volume was then reduced and hexane was added to precipitate a yellow solid. This yellow product was recrystallized from dichloromethane and hexane to yield yellow crystals of pure **3b** (52 mg, 51%). Anal. Calc. for $C_{42}H_{43}ClO_3OsP_2Si$: C, 55.34; H, 4.75. Found: C, 55.07; H, 4.78%. IR (cm^{-1}): 1904 $\nu(CO)$. 1H NMR ($CDCl_3$, δ): 0.05 (s, 3H, $SiCH_3$), 0.86 (t , 6H, $^3J_{HH}=7.0$ Hz, $Si(OCH_2CH_3)_2$), 3.36 (q, 4H, $^3J_{HH}=7.0$ Hz, $Si(OCH_2CH_3)_2$), 7.31–7.71 (m, 30H, PPh_3). ^{13}C NMR ($CDCl_3$, δ): 3.8 (s, $SiCH_3$), 17.8 (s, $Si(OCH_2CH_3)_2$), 58.1 (s, $Si(OCH_2CH_3)_2$), 127.9 (t' , $^{2,4}J_{CP}=9.0$ Hz, $o-C_6H_5$), 130.0 (s, $p-C_6H_5$), 132.7 (t' , $^{1,3}J_{CP}=50.2$ Hz, $i-C_6H_5$), 134.8 (t' , $^{3,5}J_{CP}=11.0$ Hz, $m-C_6H_5$), 182.9 (t , $^2J_{CP}=8.6$ Hz, CO).

4.8. Preparation of $Os(SiMe[OEt]_2)Cl(CO)_2(PPh_3)_2$ (**4b**)

Ethanol (2 mL) was added to an orange solution of $Os(SiMeCl_2)Cl(CO)(PPh_3)_2$ (207 mg, 0.25 mmol) in dichloromethane (20 mL). The solution turned yellow immediately, and it was stirred for 5 min. CO was then bubbled into the solution until it turned colourless. The solution was stirred for 5 min more, then concentrated, and finally hexane was added to give a white solid. This product was recrystallized from dry benzene and hexane to give pure **4b** as colourless crystals (208 mg, 91%). Anal. Calc. for $C_{42}H_{43}ClO_3OsP_2Si$: C, 55.34; H, 4.75. Found: C, 55.21; H, 4.59%. IR (cm^{-1}): 1959, 2018 $\nu(CO)$. 1H NMR ($CDCl_3$, δ): 0.01 (s, 3H, $SiCH_3$), 0.88 (t , 6H, $^3J_{HH}=6.9$ Hz, $Si(OCH_2CH_3)_2$), 2.82–2.90 (m, 2H, $Si(OCH_2CH_3)_2$), 3.24–3.32 (m, 2H, $Si(OCH_2CH_3)_2$), 7.35–7.91 (m, 30H, PPh_3). ^{13}C NMR ($CDCl_3$, δ): -1.4 (s, $SiCH_3$), 18.0 (s, $Si(OCH_2CH_3)_2$), 58.7 (s, $Si(OCH_2CH_3)_2$), 127.7 (t' , $^{2,4}J_{CP}=9.0$ Hz, $o-C_6H_5$), 129.8 (s, $p-C_6H_5$), 134.8 (t' , $^{1,3}J_{CP}=53.4$ Hz, $i-C_6H_5$), 134.2 (t' , $^{3,5}J_{CP}=9.0$ Hz, $m-C_6H_5$), 177.4 (t , $^2J_{CP}=6.0$ Hz, CO), 180.4 (t , $^2J_{CP}=9.6$ Hz, CO).

4.9. Preparation of $Ru(SiMeCl_2)Cl(CO)(PPh_3)-(\kappa^2(N,N)-NC_9H_6NH_2-8)$ (**5a**)

Under nitrogen, 8-aminoquinoline (29.5 mg, 0.20 mmol) and NEt_3 (27.9 μ L) were added to a yellow solution of $Ru(SiMeCl_2)Cl(CO)(PPh_3)_2$ (161 mg, 0.20 mmol) in benzene (20 mL) to produce an orange suspension. This was stirred for 30 min and the volatiles were then removed in vacuo, leaving a red residue. This was extracted by toluene, the orange extract was concentrated, and hexane then added to give pure **5a** as orange crystals

(107 mg, 78%). Anal. Calc. for $C_{29}H_{26}N_2Cl_3OPRuSi_3/4C_7H_8$: C, 54.55; H, 4.28; N, 3.71. Found: C, 54.46; H, 4.25; N, 4.03%. IR (cm^{-1}): 1944 $\nu(CO)$. 1H NMR (CD_2Cl_2 , δ): 0.35 (s, 3H, SiMe), 3.99 (d, 1H, $^2J_{HH}=12.0$ Hz, NH_2), 4.44 (d, 1H, $^2J_{HH}=12.0$ Hz, NH_2), 7.10–7.90 (m, 19H, C_9H_6N and PPh_3), 8.32 (apparent dd, 1H, $J_{HH}=1.4$, 8.4 Hz, C_9H_6N), 9.26–9.28 (m, 1H, C_9H_6N). ^{13}C NMR (CD_2Cl_2 , δ): 15.2 (SiMe), 123.3 (C_9H_6N), 127.7 (C_9H_6N), 127.8 (C_9H_6N), 128.8 (d, $^2J_{CP}=10.1$ Hz, $o-C_6H_5$), 129.2 (C_9H_6N), 130.2 (C_9H_6N), 130.6 ($p-C_6H_5$), 134.2 (d, $^3J_{CP}=10.1$ Hz, $m-C_6H_5$), 134.7 (d, $^1J_{CP}=48.3$ Hz, $i-C_6H_5$), 137.6 (C_9H_6N), 137.9 (C_9H_6N), 147.2 (C_9H_6N), 154.5 (C_9H_6N), 204.5 (d, $^2J_{CP}=17.1$ Hz, CO).

4.10. Preparation of $Os(SiMeCl_2)Cl(CO)(PPh_3)(\kappa^2(N,N)-NC_9H_6NH_2-8)$ (**5b**)

Under nitrogen, 8-aminoquinoline (13.4 mg, 0.091 mmol) and NEt_3 (12.7 μL) were added to a yellow solution of $Os(SiMeCl_2)Cl(CO)(PPh_3)_2$ (76 mg, 0.091 mmol) in benzene (20 mL) to produce an orange suspension. This was stirred for 30 min and the volatiles were then removed in vacuo, leaving a red residue. This was extracted by toluene, the orange extract was concentrated, and hexane then added to give pure **5b** as orange crystals (54 mg, 76%). Satisfactory elemental analyses were not obtained for this compound because of its extreme moisture sensitivity. However, the spectroscopic data for this compound are very similar to that found for the ruthenium analogue and the bis(ethoxy)-derivative (**6b**) described below was fully characterized. IR (cm^{-1}): 1892 $\nu(CO)$. 1H NMR (CD_2Cl_2 , δ): 0.36 (s, 3H, SiMe), 3.95 (d, 1H, $^2J_{HH}=11.6$ Hz, NH_2), 4.82 (d, 1H, $^2J_{HH}=12.4$ Hz, NH_2), 7.23–7.89 (m, 19H, C_9H_6N and PPh_3), 8.35 (apparent dd, 1H, $J=1.3$, 8.4 Hz, C_9H_6N), 9.35–9.38 (m, 1H, C_9H_6N). ^{13}C NMR (CD_2Cl_2 , δ): 14.4 (SiMe), 123.9 (C_9H_6N), 128.0 (C_9H_6N), 128.2 (C_9H_6N), 128.9 (d, $^2J_{CP}=10.1$ Hz, $o-C_6H_5$), 129.5 (C_9H_6N), 130.6 ($p-C_6H_5$), 130.7 (C_9H_6N), 134.0 (d, $^3J_{CP}=10.1$ Hz, $m-C_6H_5$), 136.6 (d, $^1J_{CP}=54.3$ Hz, $i-C_6H_5$), 137.8 (C_9H_6N), 137.9 (C_9H_6N), 147.8 (C_9H_6N), 154.7 (C_9H_6N), 185.4 (d, $^2J_{CP}=11.1$ Hz, CO).

4.11. Preparation of $Ru(SiMe[OEt]_2)Cl(CO)(PPh_3)(\kappa^2(N,N)-NC_9H_6NH_2-8)$ (**6a**)

EtOH (2 mL) was added to an orange solution of $Ru(SiMeCl_2)Cl(CO)(PPh_3)(\kappa^2(N,N)-NC_9H_6NH_2-8)$ (82 mg, 0.13 mmol) in benzene (20 mL). The reaction mixture was stirred for 30 min and then volatiles were removed in vacuo. The residue was extracted with CH_2Cl_2 , the orange extract was concentrated and hexane was added to give pure **6a** as yellow crystals (55 mg, 65%). Anal. Calc. for $C_{33}H_{36}ClN_2O_3PRuSi_1/3CH_2Cl_2$: C, 54.65; H, 5.04; N, 3.82. Found: C, 54.55;

H, 4.88; N, 4.11%. IR (cm^{-1}): 1907 $\nu(CO)$. 1H NMR (CD_2Cl_2 , δ): 0.15 (s, 3H, SiMe), 0.87 (t, 3H, $^3J_{HH}=7.0$ Hz, OCH_2CH_3), 1.18 (t, 3H, $^3J_{HH}=7.0$ Hz, OCH_2CH_3), 3.16–3.47 (m, 4H, OCH_2CH_3), 4.65 (d, 1H, $^2J_{HH}=11.4$ Hz, NH_2), 4.78 (d, 1H, $^2J_{HH}=11.2$ Hz, NH_2), 7.26–7.93 (m, 19H, C_9H_6N and PPh_3), 8.28 (apparent dd, 1H, $J=1.4$, 8.4 Hz, C_9H_6N), 9.27–9.29 (m, 1H, C_9H_6N). ^{13}C NMR (CD_2Cl_2 , δ): 0.2 (SiMe), 17.8 (OCH_2CH_3), 18.1 (OCH_2CH_3), 58.2 (OCH_2CH_3), 58.9 (OCH_2CH_3), 123.1 (C_9H_6N), 127.5 (C_9H_6N), 127.5 (C_9H_6N), 128.5 (d, $^2J_{CP}=10.1$ Hz, $o-C_6H_5$), 129.7 (C_9H_6N), 130.2 ($p-C_6H_5$), 130.3 (C_9H_6N), 134.2 (d, $^3J_{CP}=10.1$ Hz, $m-C_6H_5$), 136.7 (d, $^1J_{CP}=47.3$ Hz, $i-C_6H_5$), 137.7 (C_9H_6N), 138.3 (C_9H_6N), 147.8 (C_9H_6N), 153.6 (C_9H_6N), 205.8 (d, $^2J_{CP}=28.2$ Hz, CO).

4.12. Preparation of $Os(SiMe[OEt]_2)Cl(CO)(PPh_3)(\kappa^2(N,N)-NC_9H_6NH_2-8)$ (**6b**)

8-Aminoquinoline (38 mg, 0.26 mmol) was added to an orange solution of $Os(SiMeCl_2)Cl(CO)(PPh_3)_2$ (107 mg, 0.13 mmol) in benzene (20 mL) to produce an orange suspension. This was stirred for 15 min and then EtOH (2 mL) was added and the solution stirred for five more minutes. The volatiles were removed in vacuo, the residue extracted with benzene and the red extract was concentrated and hexane then added to give pure **6b** as a yellow solid (74 mg, 72%). Anal. Calc. for $C_{33}H_{36}ClN_2O_3OsPSi$: C, 49.96; H, 4.57; N, 3.53. Found: C, 49.97; H, 4.69; N, 3.66%. IR (cm^{-1}): 1894 $\nu(CO)$. 1H NMR (CD_2Cl_2 , δ): -0.32 (s, 3H, SiMe), 0.34 (t, 3H, $^3J_{HH}=7.0$ Hz, OCH_2CH_3), 0.75 (t, 3H, $^3J_{HH}=6.8$ Hz, OCH_2CH_3), 2.81–3.33 (m, 4H, OCH_2CH_3), 3.53 (d, 1H, $^2J_{HH}=11.2$ Hz, NH_2), 5.35 (d, 1H, $^2J_{HH}=11.6$ Hz, NH_2), 7.22 (apparent d, 1H, $J=7.3$ Hz, C_9H_6N), 7.35–7.49 (m, 10H, C_9H_6N and PPh_3), 7.73 (apparent d, 1H, $J=8.2$ Hz, C_9H_6N), 7.83–7.91 (m, 7H, PPh_3), 8.29 (apparent dd, 1H, $J=1.1$, 8.7 Hz, C_9H_6N), 9.46–9.48 (m, 1H, C_9H_6N). ^{13}C NMR (CD_2Cl_2 , δ): -0.4 (SiMe), 18.2 (OCH_2CH_3), 18.4 (OCH_2CH_3), 57.5 (OCH_2CH_3), 58.0 (OCH_2CH_3), 123.5 (C_9H_6N), 127.4 (C_9H_6N), 127.6 (C_9H_6N), 128.2 (d, $^2J_{CP}=10.1$ Hz, $o-C_6H_5$), 129.1 (C_9H_6N), 129.8 ($p-C_6H_5$), 130.6 (C_9H_6N), 134.1 (d, $^3J_{CP}=10.1$ Hz, $m-C_6H_5$), 136.5 (C_9H_6N), 136.6 (d, $^1J_{CP}=53.3$ Hz, $i-C_6H_5$), 139.6 (C_9H_6N), 148.4 (C_9H_6N), 153.2 (C_9H_6N), 189.5 (d, $^2J_{CP}=12.1$ Hz, CO).

4.13. Preparation of $Os(\kappa^3(Si,N,N)-SiMe[NH(2-C_5H_4-N)]_2)Cl(CO)(PPh_3)$ (**7b**)

2-Aminopyridine (46.4 mg, 0.24 mmol) in benzene (15 mL) was added slowly to an orange solution of $Os(SiMeCl_2)Cl(CO)(PPh_3)_2$ (103 mg, 0.12 mmol). The orange mixture turned to a yellow suspension upon stirring. This was stirred for 4 h and then filtered through Celite. The pale yellow filtrate was concentrated and hexane was

added to give a pale yellow solid. This was recrystallized from CH₂Cl₂/hexane to give pure **7b** as pale yellow crystals (67 mg, 75%). Anal. Calc. for C₃₀H₂₈N₄ClOOSi/2CH₂Cl₂: C, 46.50; H, 3.71; N, 7.11. Found: C, 46.85; H, 4.13; N, 7.49%. IR (cm⁻¹): 1900 vs ν(CO). ¹H NMR (CD₂Cl₂, δ): 0.07 (s, 3H, SiMe), 4.95 (s, 1H, NHpy), 5.18 (s, 1H, NHpy), 5.91 (apparent dt, 1H, *J*=1.1, 6.6 Hz, C₅H₄N), 6.30 (apparent d, 1H, *J*=8.3 Hz, C₅H₄N), 6.44 (apparent t, 1H, *J*=6.5 Hz, C₅H₄N), 6.58 (apparent d, 1H, *J*=8.3 Hz, C₅H₄N), 6.83 (apparent t, 1H, *J*=8.5 Hz, C₅H₄N), 7.03–7.07 (m, 1H, C₅H₄N), 7.17–7.23 (m, 9H, PPh₃), 7.54–7.59 (m, 6H, PPh₃), 8.51–8.53 (m, 1H, C₅H₄N), 9.41–9.43 (m, 1H, C₅H₄N). ¹³C NMR (CD₂Cl₂, δ): -2.2 (SiMe), 110.2 (C₅H₄N), 110.5 (C₅H₄N), 112.5 (C₅H₄N), 112.6 (C₅H₄N), 127.9 (d, ²*J*_{CP} = 10.1 Hz, *o*-C₆H₅), 129.44 (*p*-C₆H₅), 134.0 (d, ³*J*_{CP} = 10.1 Hz, *m*-C₆H₅), 136.2 (d, ¹*J*_{CP} = 53.3 Hz, *i*-C₆H₅), 138.0 (C₅H₄N), 138.4 (C₅H₄N), 148.5 (C₅H₄N), 149.3 (C₅H₄N), 164.5 (C₅H₄N), 165.9 (C₅H₄N), 186.8 (d, ²*J*_{CP} = 12.1 Hz, CO).

4.14. X-ray crystal structure determinations for complexes **3b**, **4b**, **5a**, **6c**, and **7b**

X-ray data collection was by Siemens SMART diffractometer with a CCD area detector at 150 K using graphite monochromated Mo K α radiation (λ =0.71073 Å). Data were integrated and corrected for Lorentz and polarisation effects using SAINT [26] software. Semi-empirical absorption corrections were applied based on equivalent reflections using SADABS [27]. The structures were solved by Patterson and Fourier methods and refined by full-matrix least squares on *F*² using programs SHELXS [28] and SHELXL [29]. All non-hydrogen atoms were refined anisotropically. Hydrogen atoms were located geometrically and refined using a riding model with thermal parameter 20% greater than *U*_{iso} of the carrier atom. The ethyl groups in **3b** show evidence of disorder and have been refined isotropically so that the thermal parameter takes up the disorder. The 1/2 molecule of benzene of solvation in **5a** is ordered. However, the final electron density map for **7b** contained numerous electron density peaks, clustered in one region of the unit cell. These could not be resolved sensibly into a molecule and presumably represent severely disordered dichloromethane of solvation. This density was removed using the “squeeze” function of PLATON [30] before the final refinement. Crystal data and refinement details are given in Table 1.

5. Supplementary material

Crystallographic data (excluding structure factors) for the structures reported have been deposited with

the Cambridge Crystallographic Data Centre as supplementary publication Nos. 231885–231889 for **3b**, **4b**, **5a**, **6c**, and **7b**, respectively. Copies of this information can be obtained free of charge from the Director, CCDC, 12 Union Road, Cambridge, CB2 1EZ, UK (fax: +44-1223-336-033; e-mail: deposit@ccdc.cam.ac.uk or www: <http://www.ccdc.cam.ac.uk>).

Acknowledgements

We thank the Marsden Fund administered by the Royal Society of NZ for supporting this work. We also thank the Croucher Foundation, Hong Kong, for support and for granting a Postdoctoral Fellowship to H.-W.K. We also thank the University of Auckland Research Committee for partial support of this work through grants-in-aid.

References

- [1] W. Malisch, S. Möller, O. Fey, H.-U. Wekel, R. Pikel, U. Posset, W. Kiefer, *J. Organomet. Chem.* 507 (1996) 117.
- [2] K. Hübler, P.A. Hunt, S.M. Maddock, C.E.F. Rickard, W.R. Roper, D.M. Salter, P. Schwerdtfeger, L.J. Wright, *Organometallics* 16 (1997) 5076.
- [3] C.E.F. Rickard, W.R. Roper, D.M. Salter, L.J. Wright, *J. Am. Chem. Soc.* 114 (1992) 9682.
- [4] W. Adam, U. Azzena, F. Prechtel, K. Hindahl, W. Malisch, *Chem. Ber.* 125 (1992) 1409.
- [5] G.R. Clark, C.E.F. Rickard, W.R. Roper, D.M. Salter, L.J. Wright, *Pure and Appl. Chem.* 62 (1990) 1039.
- [6] J.S. McIndoe, B.K. Nicholson, *J. Organomet. Chem.* 648 (2002) 237.
- [7] G. Thum, W. Ries, D. Greisinger, W. Malisch, *J. Organomet. Chem.* 252 (1983) C67.
- [8] W. Malisch, *Chem. Ber.* 107 (1974) 3835.
- [9] T.N. Choo, W.-H. Kwok, C.E.F. Rickard, W.R. Roper, L.J. Wright, *J. Organomet. Chem.* 645 (2002) 235.
- [10] W. Malisch, S. Möller, R. Lankat, J. Reising, S. Schmitzer, O. Fey, in: N. Auner, J. Weiss (Eds.), *Organosilicon Chemistry II From Molecules to Materials*, VCH Weinheim, Germany, 1996, p. 575.
- [11] W. Malisch, M. Vögler, D. Schumacher, M. Nieger, *Organometallics* 21 (2002) 2891.
- [12] S.T.N. Freeman, J.L. Petersen, F.R. Lemke, *Organometallics* 23 (2004) 1153.
- [13] S.M. Maddock, C.E.F. Rickard, W.R. Roper, L.J. Wright, *Organometallics* 15 (1996) 1793.
- [14] C.E.F. Rickard, W.R. Roper, D.M. Salter, L.J. Wright, *Organometallics* 11 (1992) 3931.
- [15] K. Hübler, W.R. Roper, L.J. Wright, *Organometallics* 16 (1997) 2730.
- [16] M. Albrecht, C.E.F. Rickard, W.R. Roper, A. Williamson, S.D. Woodgate, L.J. Wright, *J. Organomet. Chem.* 625 (2001) 77.
- [17] M.T. Attar-Bashi, C.E.F. Rickard, W.R. Roper, L.J. Wright, S.D. Woodgate, *Organometallics* 17 (1998) 504.
- [18] C.E.F. Rickard, W.R. Roper, S.D. Woodgate, L.J. Wright, *J. Organomet. Chem.* 609 (2000) 177.
- [19] G.J. Irvine, C.E.F. Rickard, W.R. Roper, A. Williamson, L.J. Wright, *Angew. Chem., Int. Ed.* 39 (2000) 948.

- [20] C.E.F. Rickard, W.R. Roper, A. Williamson, L.J. Wright, *Organometallics* 21 (2002) 4862.
- [21] G.R. Clark, G.J. Irvine, W.R. Roper, L.J. Wright, *J. Organomet. Chem.* 680 (2003) 81.
- [22] T. Sato, M. Okazaki, H. Tobita, H. Ogino, *J. Organomet. Chem.* 669 (2003) 189.
- [23] M. Stradiotto, K.L. Furdala, T.D. Tilley, *Chem. Commun.* (2001) 1200.
- [24] J.W. DiLuzio, L. Vaska, *J. Am. Chem. Soc.* 83 (1961) 1262.
- [25] C.E.F. Rickard, W.R. Roper, G.E. Taylor, J.M. Waters, L.J. Wright, *J. Organomet. Chem.* 389 (1990) 375.
- [26] SAINT, Area detector integration software, Siemens Analytical Instruments Inc., Madison, WI, USA, 1995.
- [27] G.M. Sheldrick, SADABS, Program for Semi-empirical Absorption Corrections, University of Göttingen, Göttingen, Germany, 1997.
- [28] G.M. Sheldrick, SHELXS, Program for Crystal Structure Determination, University of Göttingen, Göttingen, Germany, 1997.
- [29] G.M. Sheldrick, SHELXL, Program for Crystal Structure Refinement, University of Göttingen, Göttingen, Germany, 1997.
- [30] A.L. Spek, *Acta Cryst. A* 46 (1990) C34.